

# Oncolytic Adenovirus With Temozolomide Induces Autophagy and Antitumor Immune Responses in Cancer Patients

Ilkka Liikanen<sup>1</sup>, Laura Ahtiainen<sup>1</sup>, Mari LM Hirvinen<sup>1</sup>, Simona Bramante<sup>1</sup>, Vincenzo Cerullo<sup>1</sup>, Petri Nokisalmi<sup>1</sup>, Otto Hemminki<sup>1</sup>, Iulia Diaconu<sup>1</sup>, Sari Pesonen<sup>1</sup>, Anniina Koski<sup>1</sup>, Lotta Kangasniemi<sup>2</sup>, Salla K Pesonen<sup>1</sup>, Minna Oksanen<sup>1</sup>, Leena Laasonen<sup>3</sup>, Kaarina Partanen<sup>3</sup>, Timo Joensuu<sup>3</sup>, Fang Zhao<sup>4</sup>, Anna Kanerva<sup>1,5</sup> and Akseli Hemminki<sup>1-3</sup>

<sup>1</sup>Cancer Gene Therapy Group, Department of Pathology and Transplantation laboratory, Haartman Institute, University of Helsinki, Helsinki, Finland;

<sup>2</sup>Oncos Therapeutics, Ltd., Helsinki, Finland; <sup>3</sup>International Comprehensive Cancer Center Docrates, Helsinki, Finland; <sup>4</sup>Advanced Microscopy Unit, Department of Pathology, Haartman Institute, University of Helsinki, Helsinki, Finland; <sup>5</sup>Department of Obstetrics and Gynecology, HUCH, Helsinki, Finland

Oncolytic adenoviruses and certain chemotherapeutics can induce autophagy and immunogenic cancer cell death. We hypothesized that the combination of oncolytic adenovirus with low-dose temozolomide (TMZ) is safe, effective, and capable of inducing antitumor immune responses. Metronomic low-dose cyclophosphamide (CP) was added to selectively reduce regulatory T-cells. Pre-clinically, combination therapy inhibited tumor growth, increased autophagy, and triggered immunogenic cell death as indicated by elevated calreticulin, adenosine triphosphate (ATP) release, and nuclear protein high-mobility group box-1 (HMGB1) secretion. A total of 41 combination treatments given to 17 chemotherapy-refractory cancer patients were well tolerated. We observed anti- and proinflammatory cytokine release, evidence of virus replication, and induction of neutralizing antibodies. Tumor cells showed increased autophagy post-treatment. Release of HMGB1 into serum—a possible indicator of immune response—increased in 60% of treatments, and seemed to correlate with tumor-specific T-cell responses, observed in 10/15 cases overall ( $P = 0.0833$ ). Evidence of antitumor efficacy was seen in 67% of evaluable treatments with a trend for increased survival over matched controls treated with virus only. In summary, the combination of oncolytic adenovirus with low-dose TMZ and metronomic CP increased tumor cell autophagy, elicited antitumor immune responses, and showed promising safety and efficacy.

Received 13 September 2012; accepted 19 February 2013; advance online publication 2 April 2013. doi:10.1038/mt.2013.51

## INTRODUCTION

The cytotoxic mechanism of most anticancer drugs is induction of apoptosis, the resistance to which is a distinctive feature of recurrent advanced tumors. Emerging evidence indicates that both

oncolytic adenoviruses and certain chemotherapeutics can induce autophagic cell death.<sup>1-3</sup> Type II programmed cell death is characterized by increased turnover of cellular organelles leading to cell death. Recently, autophagy has been implicated as a prerequisite for immunogenic cancer cell death,<sup>4,5</sup> a phenomenon useful for induction of antitumor immunity.<sup>6</sup> It is characterized by exposure of calreticulin on the membrane of the dying tumor cell and subsequent release of danger signals such as adenosine triphosphate (ATP) and nuclear protein high-mobility group box-1 (HMGB1), resulting in activation of nearby dendritic cells.

Temozolomide (TMZ) is an alkylating agent, which has demonstrated antitumor activity in the treatment of, e.g., glioma, melanoma, and pituitary cancer. Virus-induced autophagy correlates positively with virus replication and oncolytic cell death,<sup>1,2,7</sup> however, the role of TMZ-induced autophagy remains controversial. As a single agent, TMZ-induced autophagy seems to have a cytoprotective role.<sup>8</sup> On the other hand, equivalent doses showed enhanced cytotoxicity through autophagy when combined with thalidomide; a drug proposed to affect the PI3K/Akt/mTOR pathway that plays a role in autophagy regulation.<sup>9</sup> Accordingly, autophagic cell death was recently found necessary for the antitumor effects of the TMZ/radiotherapy combination.<sup>10</sup> These data are compatible with the theory that baseline autophagy is essentially a survival process, whereas mortal autophagic flux—most easily achieved by a combination treatment—can be exploited in anticancer therapy. Both aspects have been studied in trials: autophagy inhibitor chloroquine has shown moderate efficacy in a phase III clinical trial;<sup>11</sup> meanwhile, the combination of thalidomide and TMZ has been studied in phase II trials with promising results.<sup>12,13</sup>

We hypothesized that the combination of oncolytic adenovirus and low-dose pulse of TMZ can lead to improved efficacy *via* induction of autophagy and antitumor immune responses. In addition, since it is well-established that regulatory T-cells are inhibitory for tumor immunotherapy,<sup>14</sup> we used low-dose metronomic cyclophosphamide (CP) for their selective reduction.<sup>15,16</sup>

Correspondence: Akseli Hemminki, Cancer Gene Therapy Group, Biomedicum. P.O. Box 63, University of Helsinki, Helsinki 00014, Finland. E-mail: akseli.hemminki@helsinki.fi

## RESULTS

### TMZ and CP increase efficacy of oncolytic adenovirus and promote immunogenic cancer cell death *in vitro*

Combination of oncolytic adenovirus Ad5/3-D24-GMCSF and TMZ was tested in prostate cancer PC3-MM2 and breast cancer MDA-MB-436 cell lines (Figure 1a and Supplementary Figure S1) together with 4-hydroperoxycyclophosphamide (4-HPCP), an active metabolite of the prodrug CP. The triple combination increased cell killing over chemotherapeutic agents and virus alone ( $P < 0.01$ ,  $P < 0.05$ , respectively). Combination of virus with either chemotherapeutic agent alone also increased cell killing (Supplementary Figure S1). In PC3-MM2 cells, combination of TMZ with oncolytic adenovirus indicated strong synergism as assessed by the Chou-Talalay method,<sup>17</sup> whereas 4-HPCP failed to show clear synergistic effect with virus *in vitro* (Supplementary Figure S2), which is compatible with its proposed immunological role. Nevertheless, the triple combination was synergistic at the most relevant “high fraction-affected levels” (the right edge of the graph).<sup>17</sup>

Immunogenic cell death is emerging as a potentially crucial step between innate and adaptive antitumor immune responses, and could be partially responsible for the efficacy of some chemotherapeutics.<sup>18</sup> Cancer cells undergoing immunogenic cell death first expose calreticulin on their outer plasma membrane, and next release HMGB1 and ATP to the tumor microenvironment. The triple combination of virus, TMZ, and 4-HPCP resulted in significant increase of calreticulin-positive cells followed by ATP and HMGB1 release when compared with control cells ( $P < 0.05$ ,  $P < 0.001$ ,  $P < 0.05$ , respectively) (Figure 1b). Of note, there were no signs of cytopathic effect at this time, suggesting release of danger signals before cell death and lysis.

### Increased autophagy coincides with tumor growth inhibition in combination-treated prostate tumors *in vivo*

Prostate cancer xenograft-bearing mice received Ad5/3-D24-GMCSF virus or growth medium twice intratumorally followed by intraperitoneal injections of TMZ (10 mg/kg) or saline, and CP (20 mg/kg) or saline (Figure 1c). Virus combined to TMZ showed enhanced tumor growth inhibition compared with control ( $P < 0.05$ ), and the effect was further enhanced when CP was added ( $P < 0.01$ ). As expected, subtherapeutic low-dose administration of both TMZ and CP alone did not inhibit tumor growth.

Electron microscopy on PC3-MM2 tumors revealed autophagic vacuoles in combination- and virus-treated tumor cells (Figure 1d). Of note, autophagic flux in the combination-treated cells appeared more pronounced since it was accompanied with a decrease in the numbers of mitochondria, accumulation of late autolysosomes (with degraded cytosolic material inside), and disruption of the plasma membrane. Virus progeny was observed inside some of the autophagic tumor cells and adjacent extracellular space. To further confirm these results, immunohistochemistry for microtubule-associated protein light chain 3 (LC3), an autophagosomal marker, was performed (Figure 1e). Combination-treated tumors presented a significantly higher frequency of LC3 punctate-positive cells compared with control tumors (Supplementary Figure S3), and were characterized by several autophagy-rich areas inside the tumors.

### Combination treatments are well tolerated in patients, with fewer adverse reactions when TMZ is administered after oncolytic adenovirus

A total of 17 patients with advanced solid tumors progressing after conventional therapies were treated with oncolytic adenoviruses (Supplementary Tables S1 and 2). Group 1 received low-dose TMZ (100 mg/day) for 5 days before virus, group 2 for 5–7 days before and 2 weeks after the virus, and group 3 for 7–10 days after viral treatment. In addition, low-dose metronomic oral CP (50 mg/day) was started 1 week before virus treatment and continued until progression<sup>16</sup> (Supplementary Table S2).

Treatments were well tolerated with mostly grade 1–2 adverse reactions (ARs) (Table 1). We observed grade 3 lymphopenia in 37% of all treatments, and one patient had a grade 4 decrease in leukocyte counts. Lymphopenia may in fact reflect redistribution of lymphocyte subsets to tumors following virus injection and therefore may not be an actual “adverse” reaction but rather a phenomenon contributing to efficacy.<sup>19,20</sup> When comparing to patient treatments with oncolytic adenoviruses and CP,<sup>16</sup> adding low-dose pulse of TMZ, as used here, does not appear to increase ARs; only grade 2 nausea seemed more common when TMZ was added (22 versus 11%, not significant).

Most ARs were spontaneously self-limiting. However, one potentially treatment-related event led to patient hospitalization and was therefore classified as a serious adverse event: grade 3 ileus was observed in a cholangiocarcinoma patient (Y166). Pediatric patient U157 experienced grade 3 liver transaminase increase and grade 2 hemoglobin decrease, and N21 had grade 3 abdominal pain and thrombocytopenia, which were alleviated by blood transfusions and antibiotics without need for hospitalization. There were no grade 4–5 clinical ARs.

Interestingly, the laboratory AR profile favored patients receiving TMZ after the virus treatment (Table 1; in parenthesis): grade 1–2 ARs were recorded in 94 and 83% of treatments in group 1 as opposed to only 75 and 50% in group 3 ( $P < 0.05$ ). A similar trend was also observed in grade 3–4 ARs. Given the adenovirus-mediated hepatotoxicity frequently seen in mice, liver enzyme elevations were of particular interest. Transaminase increases were more common when TMZ was given before virus, as opposed to only after virus ( $P = 0.06$ ; Table 1).

### Pro- and anti-inflammatory cytokines transiently increase when TMZ is administered before virus

Interleukin-6 and -10 showed a transient increase at day 1 post-treatment in the overall patient series ( $P < 0.05$  and  $P < 0.0001$ , respectively). When patients were grouped according to TMZ dosing, however, the highest inflammatory cytokine changes, and the only statistically significant ones, were observed in patients receiving TMZ before virus (group 1, Supplementary Figure S4). This finding is in concordance with the frequency of ARs post-treatment (Table 1).

### Treatment efficacy

Twenty-one individual treatments were evaluable by imaging, and nine by “tumor markers” present in serum. Efficacy was evaluated by comparing pre- and post-treatment computed

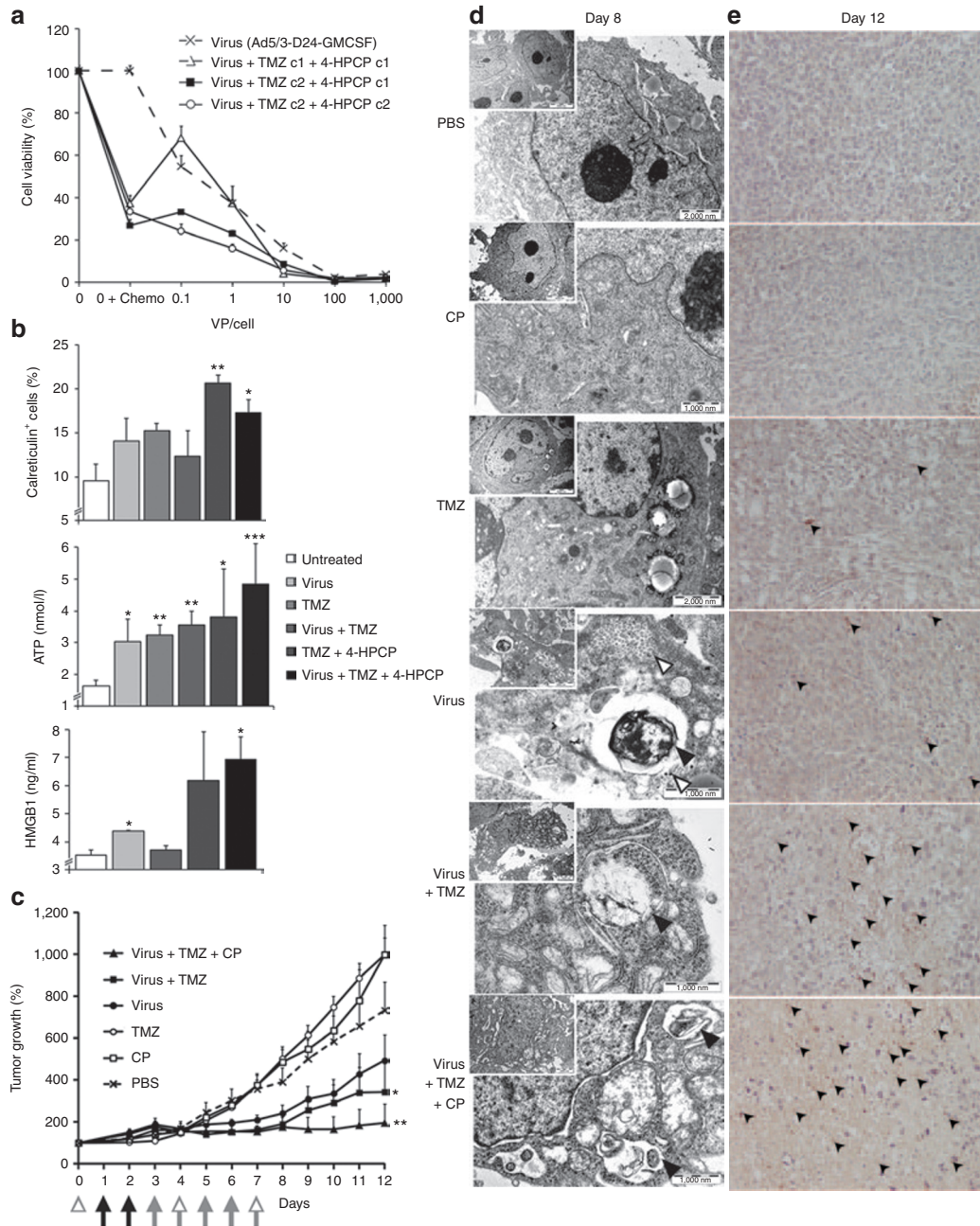


**Figure 1** Immunogenic cell killing and increased autophagy coincide with tumor growth inhibition in oncolytic adenovirus, temozolomide (TMZ)- and cyclophosphamide-treated prostate cancer. **(a)** Cell-killing efficacy of combination treatments. Ten virus particles (VP)/cell of oncolytic adenovirus combined with TMZ (c1 = 0.035, c2 = 0.105 mg/ml) and 4-HPCP (c1 = 0.003125, c2 = 0.00525 mg/ml) resulted in superior cell killing over chemotherapeutic agents or virus alone ( $P < 0.01$ ,  $P < 0.05$ , respectively). **(b)** Immunogenicity of cell death. Combination treatment with 100 VP/cell of Ad5/3-D24-GMCSF virus, TMZ (0.0025 mg/ml), and 4-HPCP (0.00208 mg/ml) resulted in significant increase in calreticulin-positive PC3-MM2 cells, and extracellular ATP and HMGB1 levels, as compared with untreated cells. Treatment with TMZ and 4-HPCP increased calreticulin-positive cells and ATP release, whereas oncolytic virus seemed to induce mostly ATP and HMGB1 release, but lacked significant induction of others. Data in **a,b** are representative of three independent experiments. **(c)** Efficacy of combination therapy *in vivo*. Nude/NMRI mice bearing subcutaneous PC3-MM2 xenografts were treated intratumorally with Ad5/3-D24-GMCSF virus or growth medium (black arrows) followed by intraperitoneal injections of TMZ or saline (gray arrows), and cyclophosphamide (CP) or saline (white arrowheads). Virus + TMZ, and virus + TMZ + CP treatments significantly inhibited tumor growth as compared with phosphate-buffered saline (PBS) control. **(d,e)** Induction of autophagy after combination therapy *in vivo*. **(d)** Electron microscopy on fixed tumor tissues revealed large tumor cells with enlarged nuclei, abundant mitochondria, ribosomes, and glycogen deposits (gray vacuoles). Autophagosomes and autolysosomes were only found in virus-, virus + TMZ-, and virus + TMZ + CP-treated tumor cells (black arrowheads). VPs were observed inside some of the autophagic cells (white arrowheads). **(e)** Tumors were assessed by immunohistochemistry for LC3, a membrane-bound protein accumulating on late autophagosomes. Punctate staining pattern was considered indicative of autophagy (black arrowheads;  $\times 40$  original magnification). Error bars represent the mean  $\pm$  SEM. All studies,  $n = 3-6$ ; \* $P < 0.05$ ; \*\* $P < 0.01$ ; \*\*\* $P < 0.001$ ; unpaired *t*-tests in **a,b**; one-way analysis of variance repeated measures in **c**. 4-HPCP, 4-hydroperoxycyclophosphamide; ATP, adenosine triphosphate; GMCSF, granulocyte-macrophage colony-stimulating factor; HMGB1, high-mobility group box-1.



**Table 1 Adverse reactions (AR) shown as a percentage of all treatments**

	Grade 1 (%)	Grade 2 (%)	Grade 3 (%)	Grade 4 (%)
<b>Laboratory</b>				
Hemoglobin decrease	34 (44; 14; 31)	22 (11; 57; 19)	0	0
Leukopenia	15 (22; 14; 6)	34 (39; 71; 13)	2 (6; 0; 0)	0
Lymphopenia	10 (11; 0; 13)	39 (44; 29; 38)	37 (28; 71; 31)	2 (6; 0; 0)
Granulocytopenia	5 (6; 0; 13)	5 (0; 0; 13)	2 (0; 14; 0)	0
Liver transaminase	27 (22; 71; 13)	10 (22; 0; 0)	2 (0; 14; 0)	0
Thrombocytopenia	27 (22; 57; 19)	2 (0; 0; 6)	2 (6; 0; 0)	0
Elevated INR	12 (17; 0; 13)	0	0	0
Hyperbilirubinemia	5 (11; 0; 0)	0	0	0
Hyponatremia	24 (33; 29; 13)	—	2 (6; 0; 0)	0
Hypokalemia	22 (22; 43; 13)	—	2 (0; 0; 6)	0
Creatinine increase	2 (6; 0; 0)	5 (6; 0; 6)	2 (0; 14; 0)	0
Any laboratory AR	88 (94; 100; 75)	71 (83; 86; 50)	49 (44; 86; 38)	2 (6; 0; 0)
<b>Pain</b>				
Injection site	15 (17; 29; 6)	5 (6; 14; 0)	0	0
Abdominal	7 (6; 29; 0)	5 (0; 14; 6)	2 (6; 0; 0)	0
Back/sides	2 (6; 0; 0)	20 (17; 57; 6)	0	0
Chest	5 (6; 14; 0)	7 (6; 29; 0)	0	0
Head	5 (0; 0; 13)	5 (0; 14; 6)	0	0
Other	17 (17; 14; 19)	5 (0; 0; 13)	0	0
<b>Gastrointestinal</b>				
Diarrhea	10 (6; 0; 19)	7 (0; 0; 19)	0	0
Constipation	5 (11; 0; 0)	2 (0; 0; 6)	0	0
Bloating	5 (0; 29; 0)	0	0	0
Dysphagia	0	5 (0; 0; 13)	0	0
Loss of appetite	5 (0; 14; 6)	5 (11; 0; 0)	0	0
Nausea	32 (33; 0; 44)	22 (22; 43; 13)	0	0
Vomiting	12 (17; 29; 0)	2 (6; 0; 0)	0	0
Ileus	0	0	2 (6; 0; 0) <sup>a</sup>	0
<b>Respiratory and cardiovascular system</b>				
Dyspnea	2 (6; 0; 0)	12 (11; 14; 13)	0	0
Cough	12 (17; 14; 6)	7 (6; 14; 6)	0	0
Hypotension	10 (11; 14; 6)	2 (6; 0; 0)	0	0
<b>General</b>				
Fever	41 (33; 43; 50)	32 (28; 43; 31)	2 (6; 0; 0)	0
Chills	41 (28; 29; 63)	15 (11; 29; 13)	0	0
Fatigue	29 (28; 57; 19)	29 (33; 43; 19)	0	0
Flu-like symptoms	7 (6; 14; 6)	2 (6; 0; 0)	0	0
Sweating	2 (6; 0; 0)	2 (6; 0; 0)	0	0
Edema/swelling	15 (11; 43; 6)	2 (0; 0; 6)	0	0
Anxiety	2 (0; 0; 6)	2 (0; 0; 6)	0	0
Any clinical AR	93 (100; 100; 81)	83 (72; 100; 88)	7 (17; 0; 0)	0
Any AR	100 (100; 100; 100)	95 (94; 100; 94)	54 (56; 86; 38)	2 (6; 0; 0)

Percentages in parentheses represent adverse reactions (ARs) in groups 1, 2, and 3, respectively. Follow-up time for ARs was 28 days after virus treatment. Grade 1–2 ARs seen in 1–2 cases are not shown. Note that the majority of grade 3–4 ARs were “lymphopenia”, which may reflect redistribution of lymphocyte subsets from blood to tumors as predicted for a potent immunotherapeutic.<sup>20</sup> Lymphocytes were manually counted utilizing leukocyte values and automated estimation of lymphocyte percentages by a clinical grade cell counter. Group 1: temozolomide before virus; Group 2: temozolomide before and after virus; Group 3: temozolomide after virus. INR, international normalized ratio.

<sup>a</sup>Serious adverse event leading to patient hospitalization, discussed in text.

**Table 2 Patient follow-up and clinical response**

Patient code	Type of cancer	Virus	Temozolomide, 100 mg/day (days)	Imaging/marker response	Survival (days)
Group 1: Temozolomide (100 mg/day) before viral treatment					
N21	Neuroblastoma	ICOVIR-7	3	US, mPR	298
H148	Pancreatic	ICOVIR-7	5	mMR	63
S149	Endometrial sarcoma	ICOVIR-7	5	SD (−5%)	951
		Ad5/3-D24-GMCSF	5	MR (−15%)	
		Ad5-D24-GMCSF	5	SD (+1%) <sup>a</sup>	
		Ad5-RGD-D24-GMCSF	5	SD (+1%) <sup>a</sup>	
		Ad5/3-D24-GMCSF	5	SD (+1%) <sup>a</sup> , mMR	
Y166	Cholangio carcinoma	Ad5/3-D24-GMCSF	5		47
N127	Head and neck	Ad5/3-D24-GMCSF	5		118
M3	Hepatocellular carcinoma	Ad5-RGD-D24-GMCSF	5		105
C156	Colon	Ad5-RGD-D24-GMCSF	5	PD (+45%) <sup>a</sup> , mPD	269
		Ad5-RGD-D24-GMCSF	5	PD (+45%) <sup>a</sup> , mPD	
		Ad5-RGD-D24-GMCSF	5	PD (+45%) <sup>a</sup> , mPD	
M50	Mesothelioma	Ad5-RGD-D24-GMCSF	5	SD (+8%)	462
		Ad5-D24-GMCSF	1	PD (+34%)	
K75	Lung adenocarcinoma	Ad5-D24-GMCSF	5		123
S119 <sup>b</sup>	Sarcoma	Ad5-D24-GMCSF	5	SD (+1%)	1,459 <sup>c</sup>
		Ad5/3-D24-GMCSF	5	SD (+12%)	
Group 2: Temozolomide (100 mg/day) before and after viral treatment					
C145	Colon	Ad5/3-D24-GMCSF	5 + 14	PD (+45%), mPD	140
		Ad5-D24-GMCSF	5 + 14	PD (+35%), mPD	
M137	Mesothelioma	Ad5-RGD-D24-GMCSF	7 + 14	SD (−4%)	779
		Ad5-D24-GMCSF	7 + 14	SD (+19%)	
U157	Wilms' tumor	Ad5/3-D24-GMCSF	5 + 0		147
		Ad5-D24-GMCSF	0 + 17		
T19	Medullary thyroid	Ad5-D24-GMCSF	5 + 15	SD (+7%), mSD	565
Group 3: Temozolomide (100 mg/day) after viral treatment					
K152	Lung adenocarcinoma	ICOVIR-7	7	PD (+35%) <sup>a</sup>	283
		Ad5/3-Cox2L-D24	7	PD (+35%) <sup>a</sup>	
		Ad5-D24-GMCSF	7	PD (+35%) <sup>a</sup>	
		Ad5-RGD-D24-GMCSF	7	PD (+48%) <sup>a</sup>	
		Ad5/3-D24-GMCSF	7	PD (+48%) <sup>a</sup>	
S153	Synovial sarcoma	Ad3-hTERT-E1A	7	PD (+48%) <sup>a</sup>	51
		Ad5/3-D24-GMCSF	10		
S171	MFH sarcoma	ICOVIR-7	10	SD (−2%)	553
		Ad5/3-D24-GMCSF	10	SD (−0%)	
		Ad3-hTERT-E1A	10	SD (−1%)	
		Ad5/3-hTERT-E1A-CD40L	10	PD (+31%) <sup>a</sup>	
		Ad5/3-hTERT-E1A-CD40L	10	PD (+31%) <sup>a</sup>	
S119 <sup>b</sup>	Sarcoma	Ad5/3-hTERT-E1A-CD40L	10	PD (+31%) <sup>a</sup>	1,459 <sup>c</sup>
		Ad3-hTERT-E1A	7	SMD (+26%) <sup>a</sup>	
		ICOVIR-7	7	SMD (+26%) <sup>a</sup>	
		Ad5-D24-GMCSF	7	SMD (+26%) <sup>a</sup>	

Percentages in parentheses indicate exact change in the sum of tumor diameters. Tumor markers (mPR, mMR, mSD, mPD), when available, were scored with the same percentages.

GMCSF, granulocyte-macrophage colony-stimulating factor; MFH, malignant fibrous histiocytoma; MR, minor response; PD, progressive disease; PR, partial response; SD, stable disease; SMD, stable metabolic disease; US, response in ultrasound imaging.

<sup>a</sup>Serial treatment, imaging was performed after the third treatment. <sup>b</sup>Patient received treatments according to group 1 and later group 3. <sup>c</sup>Alive at the end of follow-up.

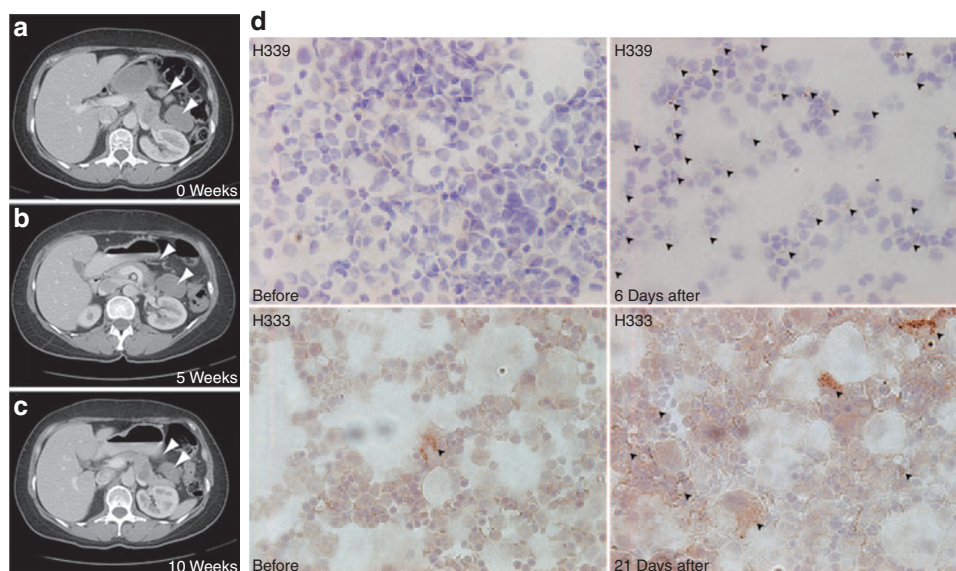


**Figure 2** Computed tomography of an endometrial sarcoma patient, and autophagy induction in patient ascites tumor cells after combination treatment. **(a–c)** Metastases near the pancreas (white arrowheads) **(a)** before treatment, and injected target lesions **(b)** after the first round of oncolytic virotherapy together with metronomic cyclophosphamide (CP), and temozolomide (TMZ) for 5 days before virus resulted in 5% decrease in tumor diameters. **(c)** Second treatment with Ad5/3-D24-GMCSF, metronomic CP, and TMZ for 5 days before virus resulted in 15% reduction. **(d)** Pre- and post-treatment ascites cells of two pancreatic carcinoma patients treated with Ad5/3-hTERT-E1A-CD40L virus, metronomic CP, and TMZ for 7 days after virus were assessed for autophagy by LC3 immunohistochemistry. Higher frequency of LC3 punctate-positive tumor cells (black arrowheads) was observed in post-treatment samples (right column) indicative of autophagy induction. No clinical information was available for these patients and therefore they are not included in the other display items. GMCSF, granulocyte-macrophage colony-stimulating factor.

tomography, magnetic resonance imaging or positron emission tomography scans. One treatment response was graded as minor response, 12 as stable disease (SD), and seven as progressive disease (**Table 2**).

An endometrial sarcoma patient S149, receiving TMZ according to group 1, benefited from the first round of combination treatment with SD and received four further treatment rounds (**Table 2**). Interestingly, the second treatment with Ad5/3-D24-GMCSF virus together with TMZ and CP resulted in 15% decrease (minor response) of the intra-abdominal lesions near the pancreas (**Figure 2a–c**). A serial combination treatment 6 months later resulted in SD and she survived for 951 days which is unusual for patients with metastatic and progressing chemotherapy-refractory grade 3 endometrial sarcoma.

Similarly, a mesothelioma patient M137 who received TMZ according to group 2, benefited from two rounds of combination treatment with sustained SD and an unexpectedly long survival of 779 days, again unusual for mesothelioma progressing after chemotherapy. Clinical benefit was suggested also by a decrease in pleural effusion. In group 3, patient S171 with malignant fibrous histiocytoma progressing at baseline, received multiple rounds of treatment with continued evidence of disease control and survival of 553 days. Pediatric patient N21 (group 1) with neuroblastoma had a partial response as assessed by tumor markers and clinical response by ultrasound imaging.

To conclude, objective evidence of efficacy, SD or better in patients progressing before therapy, was seen in 67% of radiologically evaluable treatments and in 4/9 treatments evaluable with tumor markers measured from blood.

### Presence of viral genomes and neutralizing antibodies in patient serum

Since injected virus is rapidly cleared from the circulation, extended presence of virus genomes in serum is indicative of virus replication.<sup>21</sup> We detected viral DNA in serum samples of 28/38 evaluable treatment cycles, with prolonged circulating viral DNA in 14 cases, suggesting effective virus replication (**Supplementary Table S3**). The longest timepoint for detectable virus in circulation was day 74 for pediatric patient N21. The highest titer of 611,235 virus particle (VP)/ml was observed in patient C156 after the third treatment with Ad5-RGD-D24-GMCSF virus and TMZ. Interestingly, this adenoviral capsid-specific neutralizing antibody titer had gradually increased to 1,024 (**Supplementary Table S4**), but did not seem to limit virus replication. Overall neutralizing antibodies elevated to a median of 4,096 by 1 month post-treatment. Patients who had not received prior virotherapy showed significantly lower neutralizing antibody titers at baseline and at 1 week after the first treatment ( $P < 0.05$ , both), increasing to the overall median by 1 month.

### Autophagy induction in patient ascites tumor cells after combination treatment

We had access to pre- and post-treatment ascites samples of two pancreatic carcinoma patients, who were combination-treated with oncolytic adenovirus, metronomic CP, and TMZ for 7 days after the virus, and assessed them for autophagy by LC3 immunohistochemistry. A clear increase in LC3 punctate pattern-positive tumor cells was observed 6 days after virus treatment (H339; **Figure 2d**), and still at day 21 post-treatment (H333; **Figure 2d**), indicative of autophagy induction in patients after combination therapy.

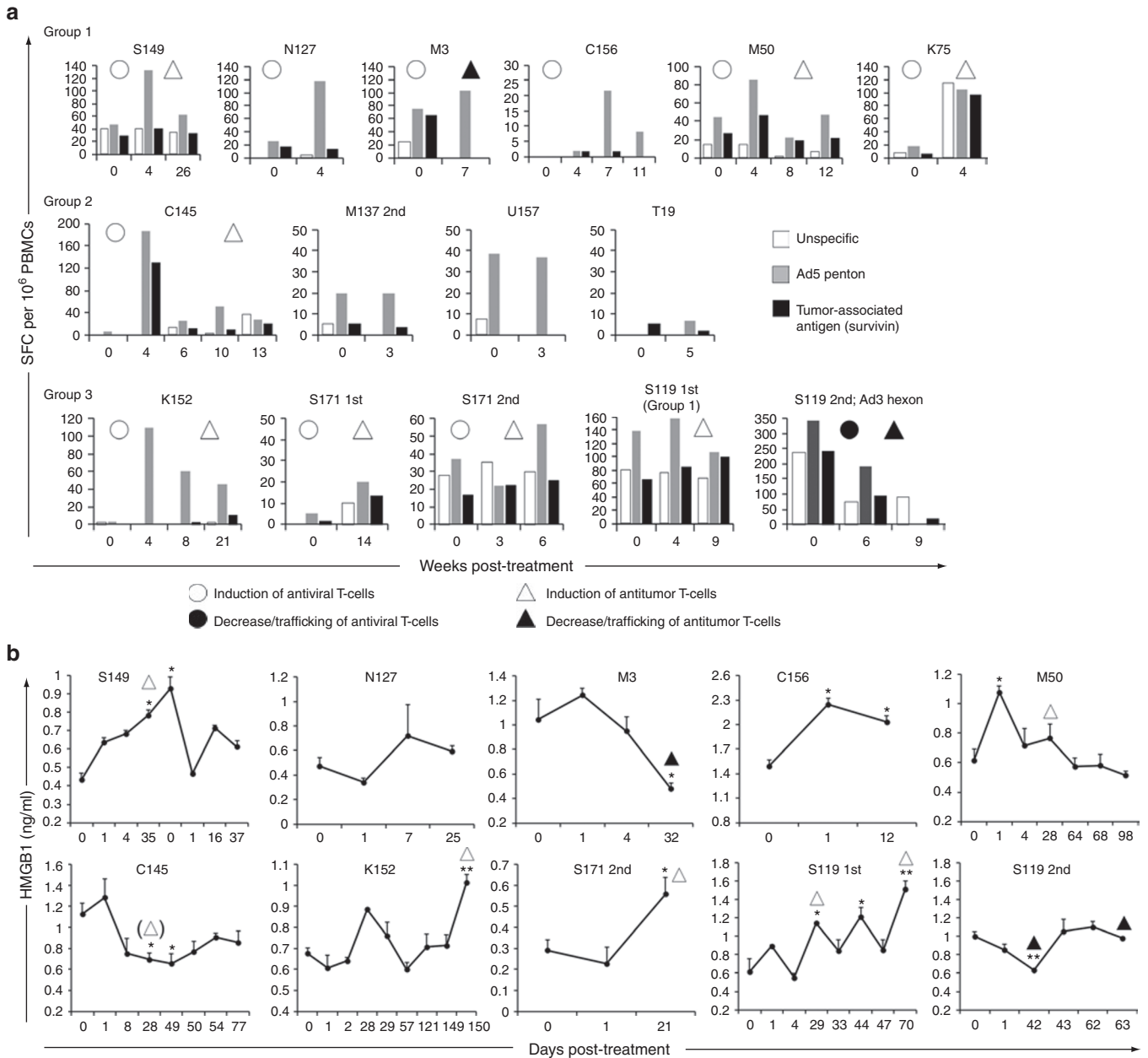


**Figure 3** Antitumor T-cells are stimulated by combination treatments and correlate with HMGB1 secretion into serum; a potential marker of immunogenic cell death. **(a)** Peripheral blood mononuclear cells (PBMCs) were pulsed with peptide mix for adenovirus serotype 5 (Ad5) penton (gray bars) or for survivin (black bars), a ubiquitous tumor-associated antigen, and assessed for T-cell activation by interferon- $\gamma$  ELISPOT analysis. Unspecific T-cell responses were also observed, which might include other tumor epitope-directed T-cells (white bars). Induction of antitumor T-cells was observed in eight cases (open triangles) and decrease/trafficking in two cases (closed triangles). Adenovirus-specific T-cell activations were seen in 10/15 cases (open circles). Patient S119 received temozolomide (TMZ) according to group 1 and later group 3; for convenience, both are shown in the group 3 row. The adenoviral peptide mix was for serotype 3 in the latter case (Ad3 hexon). **(b)** Quantitative determination of HMGB1 in patient serum was performed by enzyme-linked immunosorbent assay. Significant elevations of the immunogenic signal over baseline were observed in 60% of patients (\* $P < 0.05$ ; \*\* $P < 0.01$ ; unpaired  $t$ -test). HMGB1 titer change correlated with antitumor T-cell responses (triangle markers) in 8/9 evaluable cases. The only exception was patient C145, who showed a high antitumor T-cell induction at week 4 post-treatment, but lacked HMGB1 elevation at the time (triangle in parenthesis). The nine evaluable cases were S149, N127, M3, M50, C145, K152, and S171 2nd, S119 1st, and S119 2nd treatment rounds; Patient C156 had absolute T-cell counts below the limit of reliable detection and was therefore excluded from statistical analyses. Error bars represent the mean  $\pm$  SEM,  $n = 3$  per timepoint. 1st, initial treatment rounds; 2nd, later treatment rounds; Group 1, TMZ before virus; Group 2, TMZ after virus; Group 3, TMZ after virus; HMGB1, high-mobility group box-1; SFC, spot-forming colonies.

**Adenovirus- and tumor-specific T-cell responses in combination-treated cancer patients**

Increase of tumor-specific T-cells in blood indicates activation of the adaptive immunity, whereas decrease has been proposed

compatible with trafficking of T-cells from the blood to tumors;<sup>19,20</sup> no change could indicate immunological anergy. Cases were classified as “induction” or “decrease/trafficking” when the change was >20% over the baseline (Figure 3a). A total of 10 stimulated T-cells

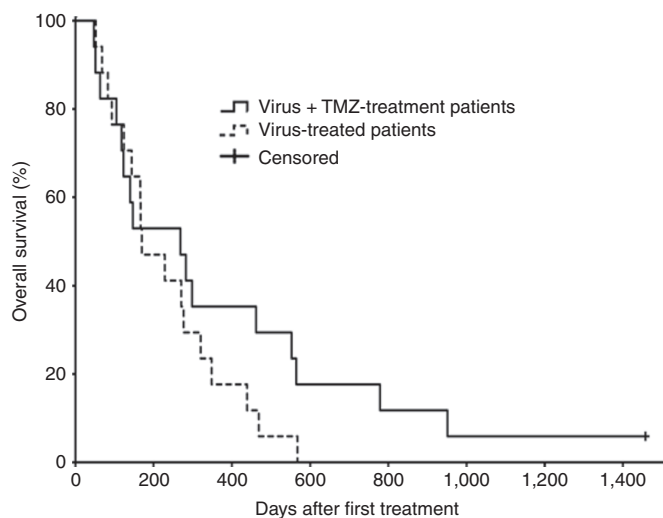


**Figure 4** Survival of combination-treated patients is increased over matched nonrandomized control patients. Overall survival of 17 oncolytic adenovirus, temozolomide (TMZ)- and cyclophosphamide (CP)-treated patients was analyzed by the Kaplan–Meier method. Matching control patients ( $n = 17$ ) treated without TMZ were selected retrospectively from the same patient cohort taking into account putative prognostic factors. Median survival in the combination-treated (Virus + TMZ) patients was 269 days versus 170 days in virus-treated controls. One combination-treated patient was alive at the end of follow-up with a survival of 1,459 days.

were considered the lower limit of reliable detection. It should be noted that cells were analyzed without prior stimulation and expansion *ex vivo*, and thus the counts represent actual numbers present in blood. Altogether 8/15 patient treatments resulted in induction of tumor-specific T-cell responses while two cases were compatible with trafficking of cells from blood to target tissues.

### Immunogenic cell death signal HMGB1 elevates in patient serum after combination treatment and correlates with tumor-specific T-cell responses

Our preclinical data suggested that cancer cell death elicited by oncolytic adenovirus together with TMZ and CP is immunogenic (Figure 1b). Thus, we hypothesized that HMGB1 in patient serum might correlate with antitumor T-cell activation; 60% of patients showed a significant elevation of HMGB1 (Figure 3b). Interestingly, the highest increase (2.5-fold) was seen in patient S119, who had prolonged disease control and the longest ongoing survival. Similarly, there was a gradual activation of antitumor T-cells by 9 weeks. It is intriguing to speculate that these two phenomena might be linked. Notably, in 8/9 evaluable cases, there was a correlation between HMGB1 titer change and antitumor T-cell response overtime ( $P = 0.0833$ ), suggesting a candidate predictive marker for antitumor immune responses, although further studies are needed in this regard.

### Survival

Overall survival of combination-treated patients was compared with nonrandomized matched control patients treated similarly in the same Advanced Therapy Access Program, but without TMZ (Figure 4). Median survival in combination-treated patients was 269 days versus 170 days in virus-only treated controls (not

significant). At the end of follow-up, one patient (S119) was still alive with 1,459 days and ongoing.

T-cell response or HMGB1 release did not correlate with therapeutic efficacy as assessed by imaging and/or tumor markers. However, Fisher's exact test suggested that there was a correlation between HMGB1 response and survival ( $P = 0.0119$ ). Six patients with HMGB1 increase had a survival higher than (or equal to) the median of the patient series, whereas three patients with decrease or no change in HMGB1 levels had shorter than median survival. When compared with matched controls, patients with HMGB1 increase had improved survival ( $P = 0.0476$ , Fisher's exact test), a provocative finding considering the lack of a significant difference in the overall population. Although tantalizing, we feel that these are quite preliminary data and should be studied further.

### DISCUSSION

Oncolytic adenoviruses are emerging as a tool for treatment of advanced solid tumors incurable with current therapies. Although safety has been excellent, the efficacy of single agent treatment leaves room for improvement.<sup>22</sup> Based on preclinical and clinical data, combination with chemotherapy has the potential to further enhance antitumor activity of oncolytic virotherapy synergistically,<sup>23–25</sup> often without an increase in side effects.

Combinations of an oncolytic virus and alkylating agents have undergone preclinical testing with favorable results.<sup>26</sup> TMZ significantly improved survival of mice when combined with oncolytic adenoviruses Ad5-D24-RGD and ICOVIR-5 in glioma xenografts,<sup>27</sup> and we saw enhanced tumor growth inhibition in prostate cancer xenografts using Ad5/3-D24-GMCSF. One poorly understood aspect of anticancer therapies in general is the mechanism of tumor cell death. “Silent” apoptotic cancer cell death—induced by most chemotherapeutics—can lead to immunological tolerance.<sup>28</sup> In contrast, emerging evidence suggests that immunogenic cancer cell death is useful or even necessary for induction of antitumor immunity.<sup>18</sup> This phenomenon has been proposed dependent on autophagy,<sup>4,5</sup> in conjunction with exposure of calreticulin on the plasma membrane and release of danger signals, ATP and nuclear protein HMGB1. Both oncolytic adenoviruses and TMZ have been shown to induce autophagic cell death in preclinical experiments.<sup>2,8,29</sup> Our data suggest that their combination increases autophagy and immunogenic cell killing in both preclinical systems and in patients, possibly in conjunction with antitumor T-cell activations observed in humans.

HMGB1 can be released from malignant cells in the context of necrotic cell death.<sup>30</sup> Preclinical studies indicate that HMGB1 levels may help in differentiating between physiological silent apoptotic cell death and pathological immunogenic necrotic, or autophagic, cell death.<sup>31</sup> Our data suggests that combination treatment results in HMGB1 release in association with autophagic cell death. A mechanistic feature could involve oncolysis, possibly enhanced by TMZ-mediated induction of autophagy, allowing leakage of HMGB1 to the systemic circulation and disclosing the current immunogenic state of the tumor. Accordingly, we noticed correlations between serum HMGB1 titer changes and antitumor T-cell responses in 8/9 evaluable treatments. This association should be studied further to determine whether HMGB1 serum level can be used as immunological response marker for



cancer therapeutics in general and oncolytic viruses in particular. Provocatively, and requiring further study, HMGB1 increase post-treatment correlated with overall survival.

Interestingly, we observed tumor- and adenovirus-specific immune responses that seemed to be enhanced in some patients by repeated combination treatment. Toll-like receptors 2 and 9 have previously been reported as the main pattern-recognition receptors for adenovirus.<sup>32,33</sup> Evidence suggests that toll-like receptor 2 is specifically recruited to the phagosomes and may be directly involved in the internalization of pathogens or their parts by cells.<sup>34</sup> In addition to non-self patterns, toll-like receptor 2 complexes are capable of detecting altered self-patterns, displayed by e.g., necrotic cells.<sup>35</sup> Therefore, pathogen recognition by immune cells may be enhanced also by autophagy-modulating agents such as TMZ.

It is noteworthy that 67% of the evaluable combination treatments resulted in disease control, taking into account that all patients were refractory to, and progressing after, available conventional treatments. Although our patient series is too small to make definitive conclusions, especially mesenchymal cancers are interesting since 80% of the instances of disease control (focusing on radiology alone: 12/13 treatments = 92%) were seen in patients with sarcoma or mesothelioma.

In conclusion, autophagy-inducing immunogenic combination treatment with oncolytic adenovirus, low-dose pulse of TMZ, and low-dose metronomic CP, given to patients with tumors refractory to conventional therapies, resulted in disease control in 67% of treatments. Safety was good throughout and liver enzyme elevations suggested that the low-dose TMZ pulse is optimally delivered after virus injections (group 3). The translational pilot investigation reported here justifies further testing and suggests that clinical trials are warranted to further study the potency of oncolytic adenoviruses with autophagy-inducing agents such as TMZ.

## MATERIALS AND METHODS

**Cell culture and viability assays.** Prostate cancer PC3-MM2 and breast cancer MDA-MB-436 cell lines (American Type Culture Collection, Manassas, VA) were cultured in Dulbecco's modified Eagle's medium (DMEM) with 10% fetal bovine serum, and maintained at humidified 37 °C and 5% CO<sub>2</sub>. Cells in triplicates were treated with Ad5/3-D24-GMCSF virus, TMZ (MSD, Espoo, Finland), and/or 4-HPCP (D-18864; NIOMECH, Bielefeld, Germany) in 100 µl of 2% DMEM, adding 100 µl of 10% DMEM 24 hours later. Cell viability was measured using CellTiter 96 Aqueous One Solution Cell Proliferation Assay (Promega, Madison, WI). To determine synergism, the interactions between Ad5/3-D24-GMCSF virus, TMZ, and 4-HPCP in PC3-MM2 cell line were analyzed with the Chou-Talalay median effect principle<sup>17</sup> using the CompuSyn software (ComboSyn, Paramus, NJ).

### Immunogenicity of cell death

**Calreticulin exposure.** PC3-MM2 cells in triplicates were infected with 100 VP/cell, and 12 hours post-infection treated with TMZ ( $c = 0.0025$  mg/ml) and/or 4-HPCP ( $c = 0.00208$  mg/ml) in 5% DMEM. Cells were harvested 24 hours later and stained with anti-calreticulin antibody (ab2907, 1:1,000; Abcam, Cambridge, UK) for 40 minutes at 4 °C and Alexa-Fluor 488 IgG as secondary antibody (A21206, 1:100; Invitrogen, Carlsbad, CA) for 40 minutes at 4 °C, and analyzed by FACSARIA flow cytometer (BD Biosciences, San Diego, CA). FlowJo software (Tree Star, Ashland, OR) was used for data analysis.

**Extracellular ATP and HMGB1.** Cells in triplicates were treated as above. Supernatant was collected after 36 hours and analyzed with ATP Determination Kit (A22066; Molecular Probes, Invitrogen, Paisley, UK) and HMGB1 ELISA Kit (ST51011; IBL International, Hamburg, Germany) according to the manufacturer's recommendations, using normal range procedure.

**Animal experiments.** Three to four weeks old male nude/NMRI mice (Taconic, Ejby, Denmark) were xenografted with  $4 \times 10^6$  PC3-MM2 cells subcutaneously in both flanks, randomized into six groups, and a week later treated twice intratumorally with  $2 \times 10^{10}$  VP of Ad5/3-D24-GMCSF virus or growth medium. Mice received intraperitoneal injections of TMZ (10 mg/kg in NaCl) or saline for five consecutive days, and CP (20 mg/kg in NaCl) or saline on days 0, 4, and 7. Tumor volume follow-up ( $n = 6$  tumors) was continued until day 12. The health of the mice was followed daily and mice were killed according to the humane end-point guidelines. Animal experiments were approved by the Experimental Animal Committee of the University of Helsinki and the Provincial Government of Southern Finland.

**Electron microscopy.** PC3-MM2 xenografts were removed immediately after euthanizing the mice and fixed with 2.5% glutaraldehyde in 0.1 mol/l phosphate buffer (pH 7.4) and post-fixed with 2% osmium tetroxide for 1 hour, dehydrated in series of ethanol, and embedded in LX-112 resin. Ultra-thin sections were cut at 50–60 nm, stained with uranyl acetate and lead citrate in Leica EMstain automatic stainer (Leica microsystems, Wetzlar, Germany) according to the manufacturer's recommendations. Imaging was performed by Jeol JEM-1400 electron microscope (Jeol, Tokyo, Japan) using 80 kV accelerating voltage. Digital microphotographs were captured by Olympus-Sis Morada digital camera (Olympus, Münster, Germany).

**Immunohistochemistry analysis.** Mouse PC3-MM2 xenografts harvested on day 12 post-treatment were fixed with 4% paraformaldehyde, embedded in paraffin, and stained with rabbit polyclonal LC3 isoform B antibody (ab48394; Abcam). Sections were boiled for 15 minutes at 98 °C in 10 mmol/l citrate buffer (pH 6) and treated with 3% hydrogen peroxide for 5 minutes. LC3B antibody (1:1,500 in Dako Antibody Diluent (S0809; Dako, Carpinteria, CA)) was applied for 60 minutes. Sections were washed and treated with LSAB+ System-HRP Kit (K0679; Dako) according to the manufacturer's instructions, and counterstained with hematoxylin. Number of LC3 punctate-positive cells (>3 dots/cell) per 40x visual field ( $n = 5$ ) was calculated under a Leica DM LB microscope, and digital images were captured using an Olympus DP50 color camera and Studio Lite 1.0 software (Pixera, San Jose, CA). For patient ascites samples, cells were fixed with methanol and assessed for immunohistochemistry as above; LC3B primary antibody (1:1,500) was applied for 120 minutes.

**Patients.** Before virotherapy, all patients had metastatic solid tumors progressing after conventional therapies with WHO performance score  $\leq 3$  and no major organ function deficiencies (**Supplementary Table S1**). Other exclusion criteria were applied as previously reported.<sup>36</sup> All patients gave a written informed consent and the principles of treatments including possible side effects were explained verbally and in writing. Treatments were given in the context of an Advanced Therapy Access Program (ATAP) regulated by Finnish Medicines Agency (FIMEA) as determined by EU/1394/2007, and performed according to Good Clinical Practice and the Helsinki Declaration of World Medical Association. Patient sample analyses are approved by the local Ethics Committee (HUS 62/13/03/02/2013).

**Adenoviruses.** All adenoviruses used in this study have been published.<sup>37–48</sup> ICOVIR-7 and Ad5-D24-RGD-GMCSF are based on serotype 5 adenovirus with a capsid modification of RGD-4C motif in the HI-loop of the fiber.<sup>37,38</sup> Ad5/3-Cox2L-D24, Ad5/3-D24-GMCSF, and Ad5/3-hTERT-E1A-CD40L are serotype 5 adenoviruses capsid-modified with adenovirus

serotype 3 knob.<sup>39–41</sup> In addition, Ad5-D24-GMCSF, Ad5/3-D24-GMCSF, and Ad5-RGD-D24-GMCSF viruses express granulocyte-macrophage colony-stimulating factor (GMCSF), and Ad5/3-hTERT-E1A-CD40L expresses human CD40 ligand.<sup>41–43</sup> Ad5/3-hTERT-E1A-CD40L and Ad3-hTERT-E1A (a serotype 3 adenovirus) have E1A under human telomerase promoter.<sup>44</sup> The tumor selectivity is based on a 24-base pair deletion in the retinoblastoma binding site of E1A or tumor-specific promoter, thus targeting replication to cancer cells. Previously published luciferase-expressing viruses Ad5LucRGD,<sup>45</sup> Ad5Luc1,<sup>46</sup> Ad5/3Luc1,<sup>47</sup> and Ad3Luc1<sup>48</sup> were used in neutralizing antibody assays. Virus production was done according to the current good manufacturing practice by Oncos Therapeutics. (Helsinki, Finland). For preclinical studies, Ad5/3-D24-GMCSF was amplified on A549 cells (American Type Culture Collection) and purified on double cesium chloride gradients. The VP concentration ( $1.6 \times 10^{13}$  VP/ml) was measured spectrophotometrically and the amount of infectious particles was determined by a standard TCID<sub>50</sub> assay on 293 cells (Microbix, Toronto, Ontario, Canada). The ratio of VP/infectious units was 18.

**Patient treatments.** Patients received oncolytic adenovirus on day 0 intratumorally (primary tumor and/or any metastasis) in ultrasound guidance, when applicable. In case of intraperitoneal or intrapleural disease, the “intratumoral” injection was performed intracavitary. Some patients received virus also intravenously, as published previously.<sup>40</sup> Patients received oral low-dose TMZ according to different dosing schedules (Supplementary Table S2): TMZ was initially administered before the virus (group 1), but due to observations of liver transaminase increase (Table 1), we aimed to assess whether combination therapy was better tolerated when TMZ was administered before and after (group 2), or only after (group 3) the virus treatment.

In the absence of contraindications (95% of treatments), patients received concomitant low-dose CP to reduce regulatory T-cells,<sup>16</sup> which was administered either metronomically per oral, as a bolus infusion together with virus injection, or as combination of these (Supplementary Table S2). Oral CP was initiated 1 week before virus treatment and continued until progression. Intravenous infusion of CP has been shown to induce similar immunological effects.<sup>16</sup> Chemotherapeutic doses were adjusted for pediatric patients (Supplementary Table S2). In ATAP, each treatment is individually optimized for each patient, and thus new information regarding the experimental therapy may have supported multiple treatment rounds, use of a different virus, or alternate dosing schedule, as in the case of patient S119 (Table 2 and Supplementary Table S2).

**Surveillance.** Patients were monitored for 24 hours in the hospital and 4 weeks as outpatients, with clinical status and laboratory data recorded intermittently. ARs were reported according to Common Terminology Criteria for Adverse Events (CTCAE) v3.0 criteria (Table 1). Pre-existing symptoms were not listed unless worsened, in which case they were scored according to final severity, not change. All grade 3–5 ARs were classified as either being serious adverse events (resulting in hospitalization, malformation, life-threatening condition, or death of patient), or not.

Tumor assessment by contrast-enhanced computed tomography, positron emission tomography-computed tomography, or magnetic resonance imaging scanning was performed before and 3–6 weeks after the treatment. In case of a serial treatment, which comprises three consecutive treatment cycles at 1-month intervals, radiological evaluation was performed before and after the complete treatment series (Table 2). RECIST v1.1 criteria<sup>49</sup> were applied to overall disease status including injected and noninjected lesions: complete response; partial response ( $\geq 30\%$  reduction in the sum of tumor diameters); SD (no response, no progression); progressive disease ( $\geq 20\%$  increase or appearance of new metastatic lesions). In addition, minor response (10–29% reduction) was used as an indicator of cases where biological activity might be present. Tumor markers, if elevated at baseline, were recorded and evaluated using the same percentages by comparing baseline to the best/worst response (Table 2).

Patient follow-up started on the virus injection day of the first TMZ-combined treatment. Matching control patients treated without TMZ were selected retrospectively among the same ATAP cohort according to the known prognostic factors in descending order of relevance (percentage of successful matches in parenthesis): tumor type (100%), concomitant low-dose CP administration (yes/no 94%), exact same round of virus treatment (71%), treatment with the same oncolytic adenovirus (52%), WHO performance status at baseline (48%). In addition, treatment dose was matched. Self-controls were not allowed.

**Detection of viral DNA in serum.** Total DNA from serum was extracted using carrier DNA (polydeoxyadenylic acid; Roche, Mannheim, Germany) with QIAamp DNA mini kit (Qiagen, Hilden, Germany), eluted in 60  $\mu$ l nuclease-free water and DNA concentration was measured by spectrophotometry. Detection of serotype 5 adenoviruses was done as described earlier.<sup>41,43,50</sup> For Ad3-hTERT-E1A virus, PCR amplification was based on a forward primer (5'-GTTTACGTG GAGGTTTCGATT-3') targeting the wild-type genome in front of the E1A promoter area, and a reverse primer (5'-GACAGCGCAGCGATCA-3') overlapping with the hTERT insertion specific to Ad3-hTERT-E1A virus. The TAMRA probe (5'-TCCGCGTACGGTGTCAAAGTTCTG-3') attaches to wild-type genome between the primers (Oligomer, Helsinki, Finland). The real-time PCR conditions for each 25  $\mu$ l reaction tested in duplicates were as follows: 2X LightCycler480 Probes Master Mix (Roche), 800 nmol/l forward and 1,000 nmol/l reverse primer, 200 nmol/l probe, and 9.5  $\mu$ l extracted DNA. Cycling conditions (Light Cycler 480; Roche): 2 minutes at 50 °C, 10 minutes at 95 °C, 50 cycles of 10 seconds at 95 °C and 1 minute at 60 °C, 10 minutes at 40 °C. TaqMan exogenous internal positive control reagents (Applied Biosystems, Carlsbad, CA) were used in the same PCR runs to test the presence of PCR inhibitors. The viral loads in serum were calculated using a regression standard curve based on serial dilutions of adenoviruses in normal human serum ( $1 \times 10^9$ – $1 \times 10^1$  VP/ml). The limit of quantification for the assay was set to 500 VP/ml of serum.

**Cytokine analysis.** Cytokine analysis was performed using BD Cytometric Bead Array Human Soluble Protein Master Buffer Kit for serum samples and BD Cytometric Bead Array Human IL-6, IL-8, IL-10, TNF- $\alpha$ , and GM-CSF Flex sets (BD Biosciences, San Diego, CA) according to the manufacturer's instructions. BD FACSAarray Bioanalyzer, BD FACS Array System software, and FCAP Array v1.0.2 software (BD Biosciences) were used for data analysis.

**Neutralizing antibody titer determination.** Neutralizing antibody titer using identical matching of adenovirus capsid (Ad5LucRGD,<sup>45</sup> Ad5Luc1,<sup>46</sup> Ad5/3Luc1,<sup>47</sup> and Ad3Luc1<sup>48</sup>) was done as described earlier.<sup>41</sup> The neutralizing titer was determined as the lowest degree of dilution that blocked gene transfer  $>80\%$ .

**Adenovirus- and tumor-specific T-cell responses.** Interferon- $\gamma$  ELISPOT was performed as previously described.<sup>41</sup> Peripheral blood mononuclear cells were stimulated with the human adenovirus serotype 5 penton or serotype 3 hexon peptide pool (HAdV-5 or HAdV-3; ProImmune, Oxford, UK) to detect adenovirus-specific responses, and with a tumor-associated BIRC5 PONAB peptide Survivin (ProImmune, Oxford, UK) to detect tumor-specific antigen responses. ELISPOT assays were performed without pre-stimulation or clonal expansion of peripheral blood mononuclear cells and thus results indicate the actual frequency of these cells in blood.

**HMGB1 in patient serum.** HMGB1 concentration in patient serum was measured in triplicates using HMGB1 ELISA Kit (ST51011; IBL International) according to the manufacturer's instructions, using high-sensitive range protocol. Hemolytic serum samples were considered unsuitable for testing.

**Statistical analysis.** Preclinical data were analyzed using two-tailed *t*-tests and one-way analysis of variance (SPSS v18.0; SPSS, Chicago, IL). ARs

were analyzed with two-tailed *t*-test for independent samples. Serum cytokine levels were analyzed with one-way analysis of variance on log-transformed data with Tukey's multiple comparison test. Neutralizing antibody and HMGB1 serum data were analyzed with two-tailed *t*-tests, and correlations between HMGB1 and T-cell responses, and HMGB1 response and survival with two-tailed Fisher's exact test ( $n = 9$ , both). Patient survival data was plotted into a Kaplan–Meier curve and groups ( $n = 17 + 17$ ) were compared pairwise with log-rank test.

## SUPPLEMENTARY MATERIAL

**Figure S1.** Oncolytic adenovirus combined with temozolomide or the active metabolite of cyclophosphamide increases cancer cell killing *in vitro*.

**Figure S2.** Interactions between oncolytic adenovirus, temozolomide, and cyclophosphamide show synergism *in vitro*.

**Figure S3.** Combination of oncolytic adenovirus, temozolomide, and cyclophosphamide induces autophagy *in vivo*.

**Figure S4.** Changes in cytokines in patients receiving oncolytic adenovirus, temozolomide, and cyclophosphamide.

**Table S1.** Patient demographics.

**Table S2.** Characteristics of patients and treatment protocols.

**Table S3.** Viral genomes present in patient serum.

**Table S4.** Neutralizing antibody titers in patient serum.

## ACKNOWLEDGMENTS

We thank the staff at Cancer Gene Therapy Group for expert assistance, and all Docrates and Eira hospital personnel for help and support. We thank Eeva-Liisa Eskelinen for helpful advice. This work was supported by: European Research Council, American Society of Clinical Oncology Foundation, Helsinki University Central Hospital Research Funds (EVO), Helsinki Biomedical Graduate School, Orion-Farmos Research Foundation, Ida Montin Foundation, Waldemar von Frenckell Foundation, Sigrid Juselius Foundation, Academy of Finland, Biocentrum Helsinki, Biocenter Finland, University of Helsinki, Cancer Organizations Finland; A.H. is K. Albin Johansson Research Professor of the Foundation for the Finnish Cancer Institute. O.H., I.D., S.P., and A.H. hold shares or options, and A.H. is a paid consultant in Oncos Therapeutics, Ltd. The other authors declared no conflict of interest.

## REFERENCES

- Ito, H, Aoki, H, Kühnel, F, Kondo, Y, Kubicka, S, Wirth, T *et al.* (2006). Autophagic cell death of malignant glioma cells induced by a conditionally replicating adenovirus. *J Natl Cancer Inst* **98**: 625–636.
- Jiang, H, White, EJ, Ríos-Vicil, CI, Xu, J, Gomez-Manzano, C and Fueyo, J (2011). Human adenovirus type 5 induces cell lysis through autophagy and autophagy-triggered caspase activity. *J Virol* **85**: 4720–4729.
- Chen, N and Karantza, V (2011). Autophagy as a therapeutic target in cancer. *Cancer Biol Ther* **11**: 157–168.
- Michaud, M, Martins, I, Sukkurwala, AQ, Adjemian, S, Ma, Y, Pellegatti, P *et al.* (2011). Autophagy-dependent anticancer immune responses induced by chemotherapeutic agents in mice. *Science* **334**: 1573–1577.
- Martins, I, Michaud, M, Sukkurwala, AQ, Adjemian, S, Ma, Y, Shen, S *et al.* (2012). Premortem autophagy determines the immunogenicity of chemotherapy-induced cancer cell death. *Autophagy* **8**: 413–415.
- Hannani, D, Sistigu, A, Kepp, O, Galluzzi, L, Kroemer, G and Zitvogel, L (2011). Prerequisites for the antitumor vaccine-like effect of chemotherapy and radiotherapy. *Cancer J* **17**: 351–358.
- Rodriguez-Rocha, H, Gomez-Gutierrez, JG, Garcia-Garcia, A, Rao, XM, Chen, L, McMasters, KM *et al.* (2011). Adenoviruses induce autophagy to promote virus replication and oncolysis. *Virology* **416**: 9–15.
- Kanzawa, T, Germano, IM, Komata, T, Ito, H, Kondo, Y and Kondo, S (2004). Role of autophagy in temozolomide-induced cytotoxicity for malignant glioma cells. *Cell Death Differ* **11**: 448–457.
- Gao, S, Yang, XJ, Zhang, WC, Ji, YW and Pan, Q (2009). Mechanism of thalidomide to enhance cytotoxicity of temozolomide in U251-MG glioma cells *in vitro*. *Chin Med J* **122**: 1260–1266.
- Palumbo, S, Pirtoli, L, Tini, P, Cevenini, G, Calderaro, F, Toscano, M *et al.* (2012). Different involvement of autophagy in human malignant glioma cell lines undergoing irradiation and temozolomide combined treatments. *J Cell Biochem* **113**: 2308–2318.
- Sotelo, J, Briceño, E and López-González, MA (2006). Adding chloroquine to conventional treatment for glioblastoma multiforme: a randomized, double-blind, placebo-controlled trial. *Ann Intern Med* **144**: 337–343.
- Hwu, WJ, Krown, SE, Menell, JH, Panageas, KS, Merrell, J, Lamb, LA *et al.* (2003). Phase II study of temozolomide plus thalidomide for the treatment of metastatic melanoma. *J Clin Oncol* **21**: 3351–3356.
- Chang, SM, Lamborn, KR, Malec, M, Larson, D, Wara, W, Sneed, P *et al.* (2004). Phase II study of temozolomide and thalidomide with radiation therapy for newly diagnosed glioblastoma multiforme. *Int J Radiat Oncol Biol Phys* **60**: 353–357.
- Zou, W (2006). Regulatory T cells, tumour immunity and immunotherapy. *Nat Rev Immunol* **6**: 295–307.
- Ghiringhelli, F, Menard, C, Puig, PE, Ladoire, S, Roux, S, Martin, F *et al.* (2007). Metronomic cyclophosphamide regimen selectively depletes CD4+CD25+ regulatory T cells and restores T and NK effector functions in end stage cancer patients. *Cancer Immunol Immunother* **56**: 641–648.
- Cerullo, V, Diaconu, I, Kangasniemi, L, Rajecki, M, Escutenaire, S, Koski, A *et al.* (2011). Immunological effects of low-dose cyclophosphamide in cancer patients treated with oncolytic adenovirus. *Mol Ther* **19**: 1737–1746.
- Chou, TC (2010). Drug combination studies and their synergy quantification using the Chou-Talalay method. *Cancer Res* **70**: 440–446.
- Kepp, O, Galluzzi, L, Martins, I, Schlemmer, F, Adjemian, S, Michaud, M *et al.* (2011). Molecular determinants of immunogenic cell death elicited by anticancer chemotherapy. *Cancer Metastasis Rev* **30**: 61–69.
- Kanerva, A, Nokisalmi, P, Tähtinen, S, Koski, A, Kangasniemi, L, Diaconu, I *et al.* (2012). Serial treatment with oncolytic adenovirus results in redistribution of T-cell subsets in humans and mice. *Mol Ther* **20**: Supplement 1.
- Brahmer, JR, Drake, CG, Wollner, I, Powderly, JD, Picus, J, Sharfman, WH *et al.* (2010). Phase I study of single-agent anti-programmed death-1 (MDX-1106) in refractory solid tumors: safety, clinical activity, pharmacodynamics, and immunologic correlates. *J Clin Oncol* **28**: 3167–3175.
- Galanis, E, Okuno, SH, Nascimento, AG, Lewis, BD, Lee, RA, Oliveira, AM *et al.* (2005). Phase I-II trial of ONYX-015 in combination with MAP chemotherapy in patients with advanced sarcomas. *Gene Ther* **12**: 437–445.
- Kirn, D (2001). Clinical research results with dl1520 (Onyx-015), a replication-selective adenovirus for the treatment of cancer: what have we learned? *Gene Ther* **8**: 89–98.
- Cheong, SC, Wang, Y, Meng, JH, Hill, R, Sweeney, K, Kirn, D *et al.* (2008). E1A-expressing adenoviral E3B mutants act synergistically with chemotherapeutics in immunocompetent tumor models. *Cancer Gene Ther* **15**: 40–50.
- Raki, M, Kanerva, A, Ristimäki, A, Desmond, RA, Chen, DT, Ranki, T *et al.* (2005). Combination of gemcitabine and Ad5/3-Delta24, a tropism modified conditionally replicating adenovirus, for the treatment of ovarian cancer. *Gene Ther* **12**: 1198–1205.
- Khuri, FR, Nemunaitis, J, Ganly, I, Arseneau, J, Tannock, IF, Romel, L *et al.* (2000). A controlled trial of intratumoral ONYX-015, a selectively-replicating adenovirus, in combination with cisplatin and 5-fluorouracil in patients with recurrent head and neck cancer. *Nat Med* **6**: 879–885.
- Ottolino-Perry, K, Diallo, JS, Lichty, BD, Bell, JC and McCart, JA (2010). Intelligent design: combination therapy with oncolytic viruses. *Mol Ther* **18**: 251–263.
- Alonso, MM, Gomez-Manzano, C, Jiang, H, Bekele, NB, Piao, Y, Yung, WK *et al.* (2007). Combination of the oncolytic adenovirus ICOVIR-5 with chemotherapy provides enhanced anti-glioma effect *in vivo*. *Cancer Gene Ther* **14**: 756–761.
- Green, DR, Ferguson, T, Zitvogel, L and Kroemer, G (2009). Immunogenic and tolerogenic cell death. *Nat Rev Immunol* **9**: 353–363.
- Ulasov, IV, Sonabend, AM, Nandi, S, Khramtsov, A, Han, Y and Lesniak, MS (2009). Combination of adenoviral virotherapy and temozolomide chemotherapy eradicates malignant glioma through autophagic and apoptotic cell death *in vivo*. *Br J Cancer* **100**: 1154–1164.
- Scaffidi, P, Misteli, T and Bianchi, ME (2002). Release of chromatin protein HMGB1 by necrotic cells triggers inflammation. *Nature* **418**: 191–195.
- Bianchi, ME and Manfredi, AA (2007). High-mobility group box 1 (HMGB1) protein at the crossroads between innate and adaptive immunity. *Immunol Rev* **220**: 35–46.
- Appledorn, DM, Patial, S, McBride, A, Godbehere, S, Van Rooijen, N, Parameswaran, N *et al.* (2008). Adenovirus vector-induced innate inflammatory mediators, MAPK signaling, as well as adaptive immune responses are dependent upon both TLR2 and TLR9 *in vivo*. *J Immunol* **181**: 2134–2144.
- Cerullo, V, Seiler, MP, Mane, V, Brunetti-Pierri, N, Clarke, C, Bertin, TK *et al.* (2007). Toll-like receptor 9 triggers an innate immune response to helper-dependent adenoviral vectors. *Mol Ther* **15**: 378–385.
- Schjetne, KW, Thompson, KM, Nilsen, N, Flo, TH, Fleckenstein, B, Iversen, JG *et al.* (2003). Cutting edge: link between innate and adaptive immunity: Toll-like receptor 2 internalizes antigen for presentation to CD4+ T cells and could be an efficient vaccine target. *J Immunol* **171**: 32–36.
- Jounai, N, Kobiyama, K and Takeshita, F (2012). Intracellular inflammatory sensors for foreign invaders and substances of self-origin. *Adv Exp Med Biol* **738**: 60–78.
- Koski, A, Raki, M, Nokisalmi, P, Liikanen, I, Kangasniemi, L, Joensuu, T *et al.* (2012). Verapamil results in increased blood levels of oncolytic adenovirus in treatment of patients with advanced cancer. *Mol Ther* **20**: 221–229.
- Nokisalmi, P, Pesonen, S, Escutenaire, S, Särkioja, M, Raki, M, Cerullo, V *et al.* (2010). Oncolytic adenovirus ICOVIR-7 in patients with advanced and refractory solid tumors. *Clin Cancer Res* **16**: 3035–3043.
- Pesonen, S, Diaconu, I, Cerullo, V, Escutenaire, S, Raki, M, Kangasniemi, L *et al.* (2012). Integrin targeted oncolytic adenoviruses Ad5-D24-RGD and Ad5-RGD-D24-GMCSF for treatment of patients with advanced chemotherapy refractory solid tumors. *Int J Cancer* **130**: 1937–1947.
- Pesonen, S, Nokisalmi, P, Escutenaire, S, Särkioja, M, Raki, M, Cerullo, V *et al.* (2010). Prolonged systemic circulation of chimeric oncolytic adenovirus Ad5/3-Cox2L-D24 in patients with metastatic and refractory solid tumors. *Gene Ther* **17**: 892–904.
- Koski, A, Kangasniemi, L, Escutenaire, S, Pesonen, S, Cerullo, V, Diaconu, I *et al.* (2010). Treatment of cancer patients with a serotype 5/3 chimeric oncolytic adenovirus expressing GMCSF. *Mol Ther* **18**: 1874–1884.
- Cerullo, V, Pesonen, S, Diaconu, I, Escutenaire, S, Arstila, PT, Ugolini, M *et al.* (2010). Oncolytic adenovirus coding for granulocyte macrophage colony-stimulating factor induces antitumoral immunity in cancer patients. *Cancer Res* **70**: 4297–4309.



42. Diaconu, I, Cerullo, V, Hirvonen, ML, Escutenaire, S, Ugolini, M, Pesonen, SK *et al.* (2012). Immune response is an important aspect of the antitumor effect produced by a CD40L-encoding oncolytic adenovirus. *Cancer Res* **72**: 2327–2338.
43. Pesonen, S, Diaconu, I, Kangasniemi, L, Ranki, T, Kanerva, A, Pesonen, SK *et al.* (2012). Oncolytic immunotherapy of advanced solid tumors with a CD40L-expressing replicating adenovirus: assessment of safety and immunologic responses in patients. *Cancer Res* **72**: 1621–1631.
44. Hemminki, O, Bauerschmitz, G, Hemmi, S, Lavilla-Alonso, S, Diaconu, I, Guse, K *et al.* (2011). Oncolytic adenovirus based on serotype 3. *Cancer Gene Ther* **18**: 288–296.
45. Kanerva, A, Wang, M, Bauerschmitz, GJ, Lam, JT, Desmond, RA, Bhoola, SM *et al.* (2002). Gene transfer to ovarian cancer versus normal tissues with fiber-modified adenoviruses. *Mol Ther* **5**: 695–704.
46. Krasnykh, V, Belousova, N, Korokhov, N, Mikheeva, G and Curiel, DT (2001). Genetic targeting of an adenovirus vector via replacement of the fiber protein with the phage T4 fibritin. *J Virol* **75**: 4176–4183.
47. Kanerva, A, Mikheeva, GV, Krasnykh, V, Coolidge, CJ, Lam, JT, Mahasreshti, PJ *et al.* (2002). Targeting adenovirus to the serotype 3 receptor increases gene transfer efficiency to ovarian cancer cells. *Clin Cancer Res* **8**: 275–280.
48. Fleischli, C, Sirena, D, Lesage, G, Havenga, MJ, Cattaneo, R, Greber, UF *et al.* (2007). Species B adenovirus serotypes 3, 7, 11 and 35 share similar binding sites on the membrane cofactor protein CD46 receptor. *J Gen Virol* **88**(Pt 11): 2925–2934.
49. Eisenhauer, EA, Therasse, P, Bogaerts, J, Schwartz, LH, Sargent, D, Ford, R *et al.* (2009). New response evaluation criteria in solid tumours: revised RECIST guideline (version 1.1). *Eur J Cancer* **45**: 228–247.
50. Escutenaire, S, Cerullo, V, Diaconu, I, Ahtiainen, L, Hannuksela, P, Oksanen, M *et al.* (2011). *In vivo* and *in vitro* distribution of type 5 and fiber-modified oncolytic adenoviruses in human blood compartments. *Ann Med* **43**: 151–163.